Electronic Supplementary Material (ESI) for CrystEngComm

Supplementary Information

Superparamagnetic mesoporous ferrite nanocrystal clusters for efficient removal of arsenite from water

Wei-Hong Xu, *[a] **Lei Wang,**[a] **Jing Wang,**[a] **Guo-Ping Sheng,**[b] **Jin-Huai Liu,**[a] **Han-Qing Yu**[b] **and Xing-Jiu Huang***[a]

[a]Nano-Materials and Environmental Detection Laboratory, Hefei Institute of Intelligent Machines, Chinese Academy of Sciences, Hefei, 230031, China

[b]Department of Chemistry, University of Science and Technology of China, Hefei, 230026, China

1. High Water-Dispersibility of Adsorbents

The as-prepared $MnFe_2O_4$ and calcined $MnFe_2O_4$ NCs are highly water dispersible and keep a stable dispersion for about half one day owing to the electrostatic repulsion and superparamagnetic effect. The surface of both NCs possesses positive charges under neutral conditions through zeta potential measurement because both NCs had a zero point of zeta potential at pH about 8.5 (Fig. S4). The superparamagnetic NCs do not aggregate in solution because of no magnetic interaction between each other.[1] Taking $MnFe_2O_4$ NCs as an example, the $MnFe_2O_4$ NCs were well dispersed in solution, (Fig. S5a). When a magnet (4000 Oe) was placed beside the vial, the ferrite NCs were separated from their dispersion rapidly within one minute due to the superparamagnetic property and high saturation magnetization (Fig. S5b). Once the magnet was taken away, the NCs could be re-dispersed into the solution immediately by slight shaking (Fig. S5c).

2. As(III) Adsorption Equilibrium Modeling

The Langmuir adsorption model can be represented in linear form as follows: [2]

$$\frac{1}{q_e} = \frac{1}{q_{\max} b} \times \frac{1}{C_e} + \frac{1}{q_{\max}} \qquad \text{S1}$$

where q_{e} is the equilibrium adsorption capacity (mg/g), C_{e} is the equilibrium concentration (mg/L), q_{max} represents the maximum amount of As(III) adsorbed on per unit weight of adsorbent to form a complete monolayer on the surface(mg/g), b is the Langmuir constant that directly relates to the adsorption affinity (L/mg).

Langmuir parameters, q_{max} and b are calculated from the slop and intercept of the linear plots of $1/q_e$ vs $1/C_e$ (Figs. S8 and S9).

The linear form of Freundlich adsorption model is as follows: [2]

$$\log(q_e) = \log K_f + \frac{1}{n}\log(C_e) \tag{S2}$$

where K_f and $1/n$ are Freundlich constants, related to adsorption capacity and adsorption intensity (heterogeneity factor) respectively. The values of K_f and $1/n$ are obtained from the slop and intercept of the linear Freundlich plot of $\log(q_e)$ vs $\log(C_e)$ (Figs. S8 and S9).

The D-R isotherm model can be represented in linear form as follows: [2]

$$\ln q_e = \ln Q_m - k_{ads}\varepsilon^2 \quad \text{and} \quad \varepsilon = RT\ln(1+\frac{1}{C_e}) \tag{S3}$$

where Q_m is the theoretical adsorption capacity (mg/g), K_{ads} is a constant related to adsorption energy, ε is polyani potential, R is gas constant (KJ/mol.K), T is temperature (K). The values of K_{ads} and $\ln Q_m$ are obtained from the slop and intercept of the linear D-R plot of $\ln q_e$ vs ε^2 (Figs. S8 and S9).

3. As(III) Adsorption Kinetics

The pseudo-first-order equation is generally expressed as follows: [2]

$$\log(q_e - q_t) = \log q_e - \frac{k_{ads}}{2.303}t \tag{S4}$$

where q_e and q_t (both in mg/g) are the amount of As(III) adsorbed per unit mass of adsorbent at equilibrium and time "*t*" respectively. The adsorption rate constant (k_{ads}) for As(III) sorption was calculated from the slop of the linear plot $\log(q_e\text{-}q_t)$ vs time (t) as shown in Figs. S10 and S11 and Table S2.

The pseudo-second-order model is commonly expressed as follows: [2]

$$\frac{t}{q_t} = \frac{1}{h} + \frac{t}{q_e} \qquad \text{S5}$$

where h is the initial sorption rate (mg/g min). The values of q_e (1/slope) and h (1/intercept) can be calculated from the plot of t/q_t vs t as shown in Figs. S10 and S11 and Table S2.

The intra-particle pore diffusion model can be expressed as follows:

$$q_t = k_i t^{1/2} \qquad \text{S6}$$

where k_i (mg g^{-1} min$^{1/2}$) is the intra-particle pore diffusion rate constant, q_t amount of As(III) adsorbed per unit mass of adsorbent at any time t, was plotted as a function of square root of time $t^{1/2}$ as shown in Fig. S12.

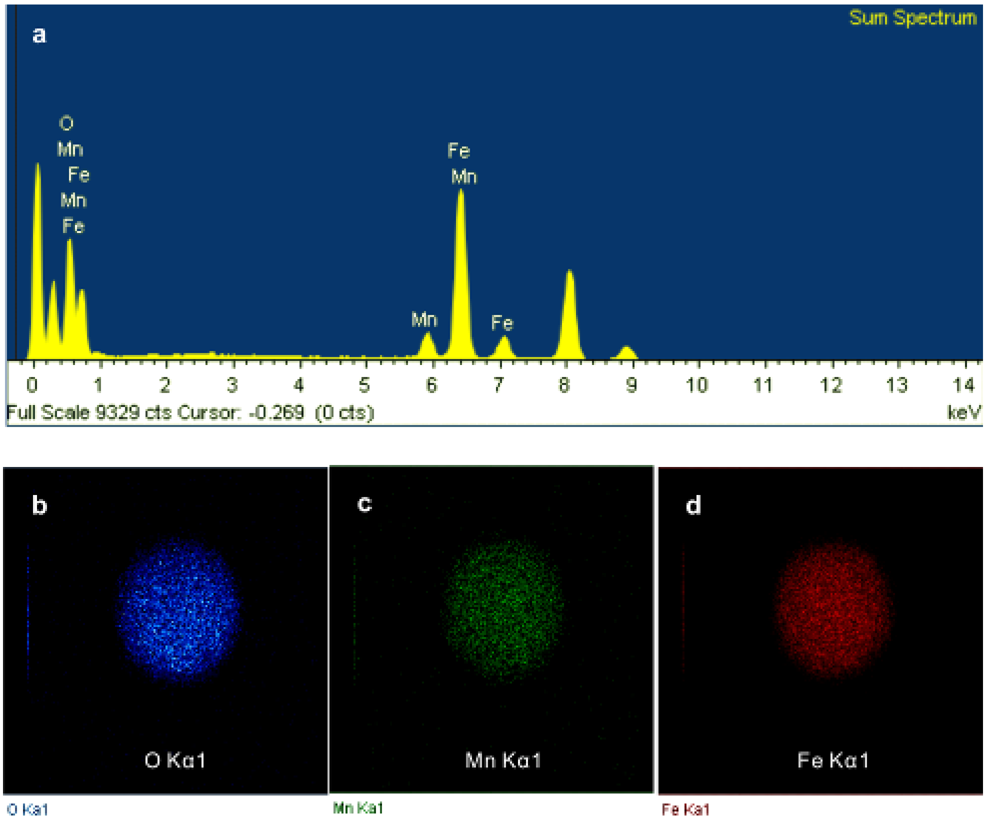

Fig. S1 a) EDX spectra of $MnFe_2O_4$ NCs; b-d) Corresponding elemental mapping of O Kα1, Mn Kα1, and Fe Kα1, respectively.

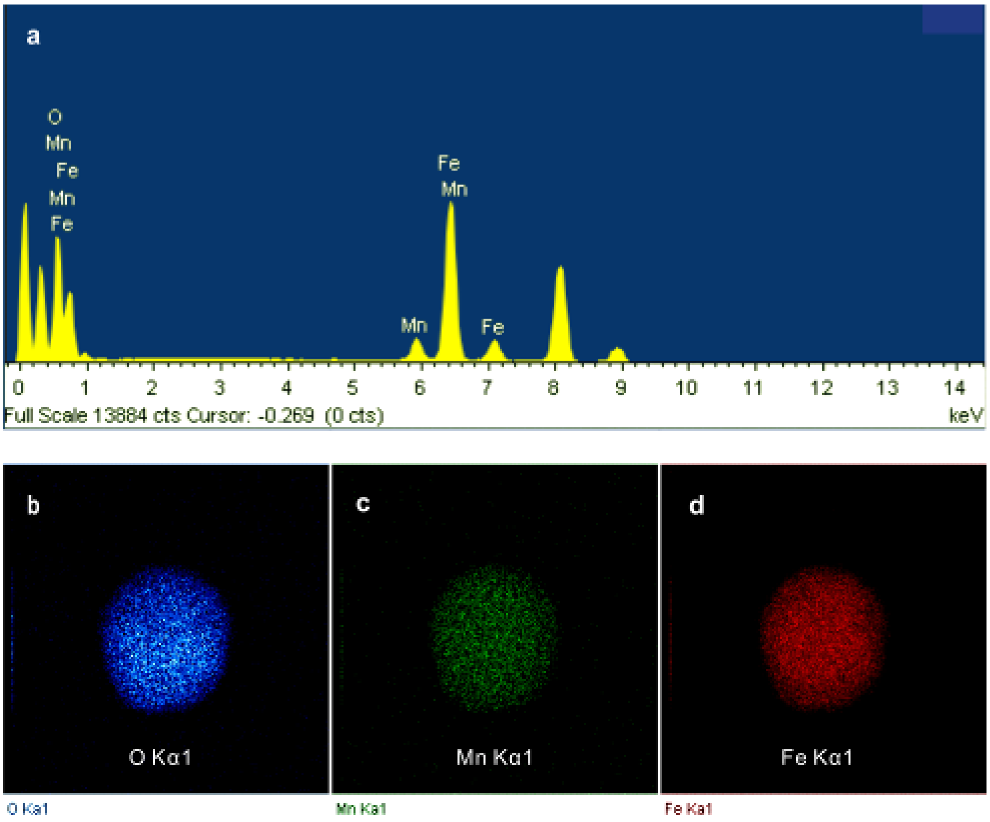

Fig. S2 a) EDX spectra of $MnFe_2O_4$ NCs calcined at 500°C in air; b-d) Corresponding elemental mapping of O Kα1, Mn Kα1, and Fe Kα1, respectively.

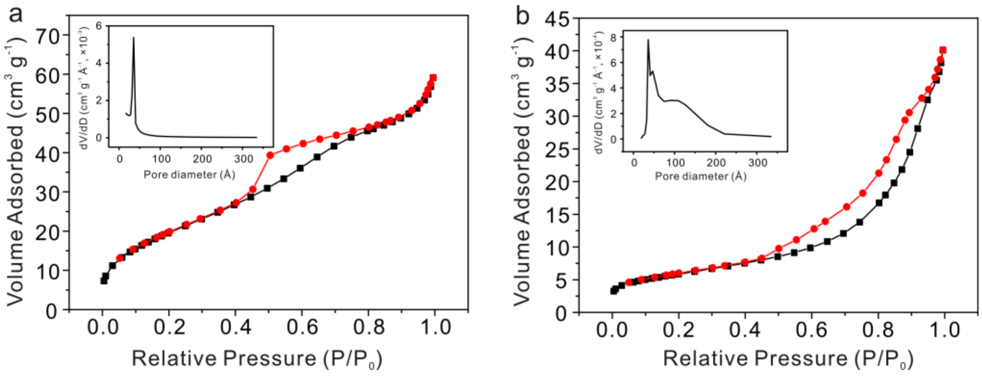

Fig. S3 N_2 sorption isotherms and pore size distribution (inset) of $MnFe_2O_4$ NCs (a) and $MnFe_2O_4$ NCs calcined at 500°C in air (b).

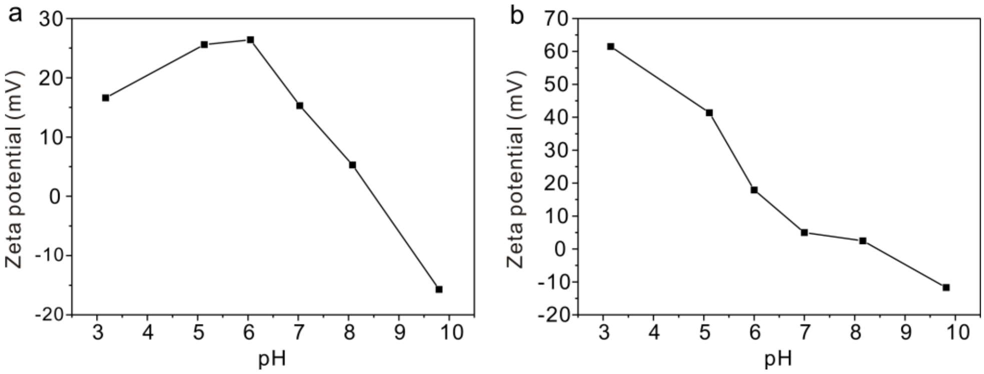

Fig. S4 Zeta potential as a function of pH. a) $MnFe_2O_4$ NCs; b) $MnFe_2O_4$ NCs calcined at 500°C in air.

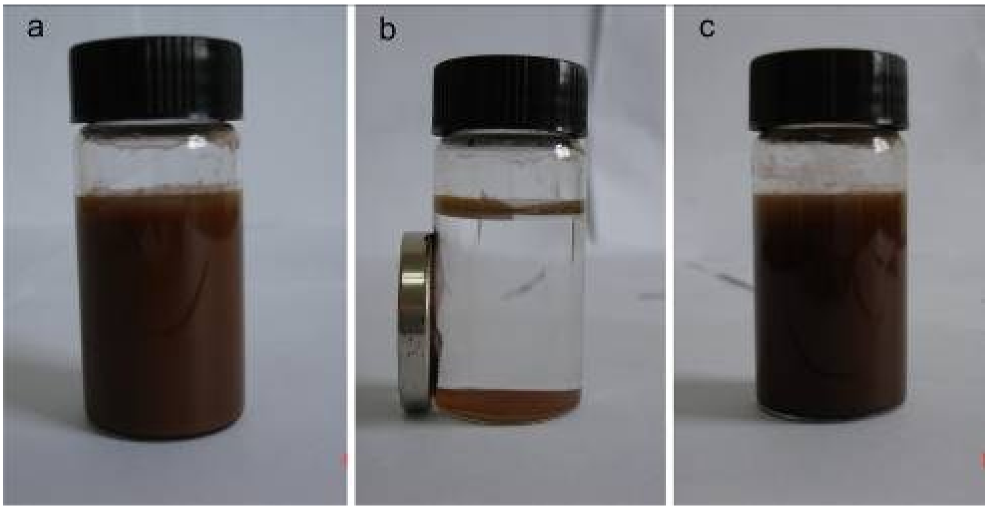

Fig. S5 Photographs of $MnFe_2O_4$ NCs dispersion in a vial. a) without magnetic field; b) with magnetic field for 1 min; c) after the magnetic field is taken away.

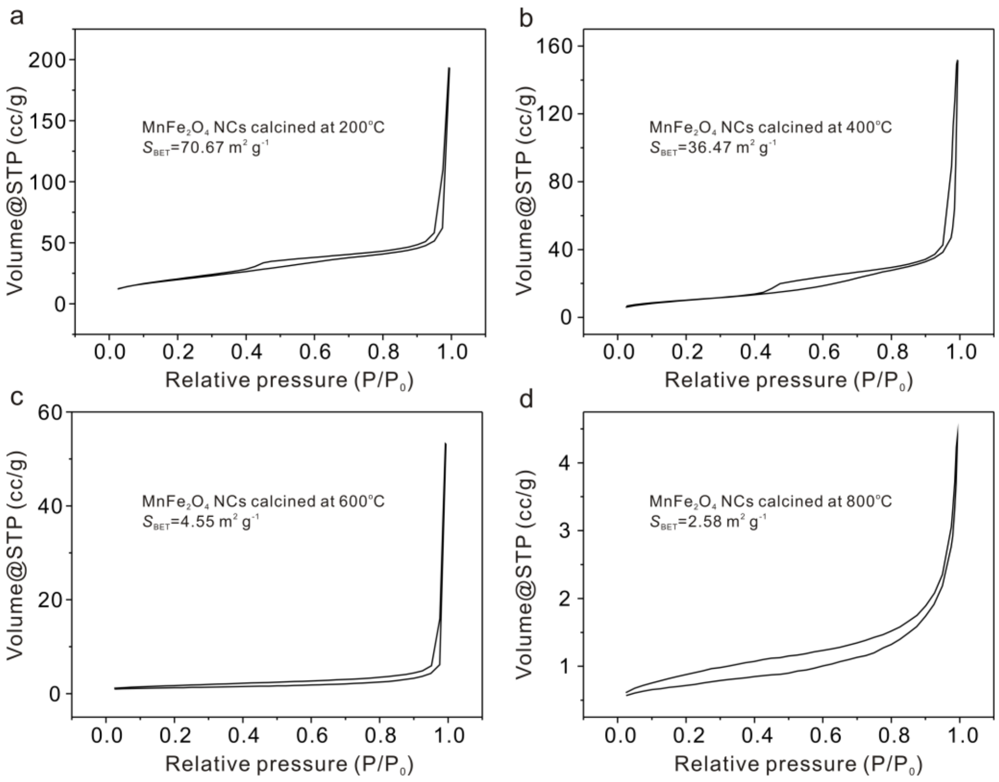

Fig. S6 N_2 sorption isotherms of $MnFe_2O_4$ NCs calcined at 200 °C (a), 400 °C (b), 600°C (c), and 800 °C (b) in air, respectively.

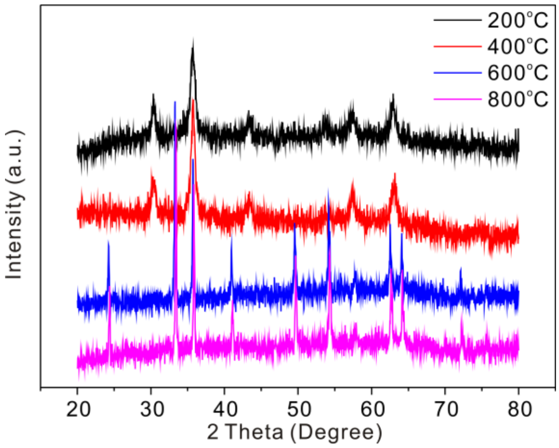

Fig. S7 XRD patterns of $MnFe_2O_4$ NCs calcined at 200°C, 400°C, 600°C, 800 °C in air, respectively.

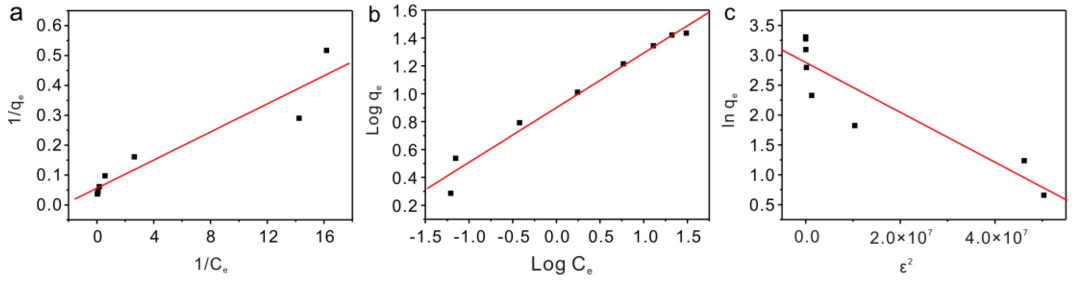

Fig. S8 Fitting of the adsorption isotherms of As(III) on the $MnFe_2O_4$ NCs by using Langmuir model (a), Freundlich model (b), and D-R isotherm model (c). The fitted parameters are summarized in Table S1.

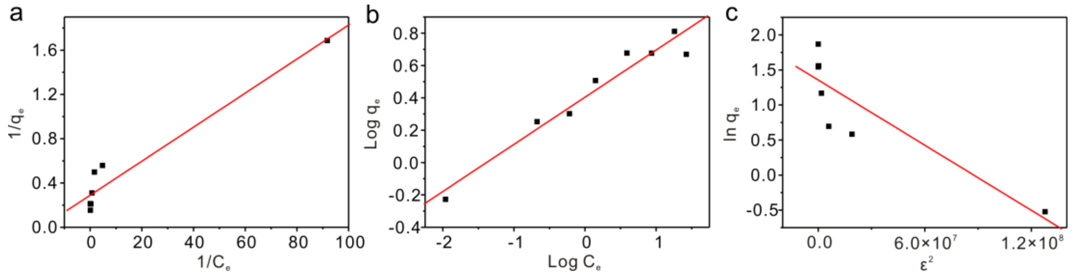

Fig. S9 Fitting of the adsorption isotherms of As(III) on the calcined $MnFe_2O_4$ NCs by using Langmuir model (a), Freundlich model (b), and D-R isotherm model (c). The fitted parameters are summarized in Table S1.

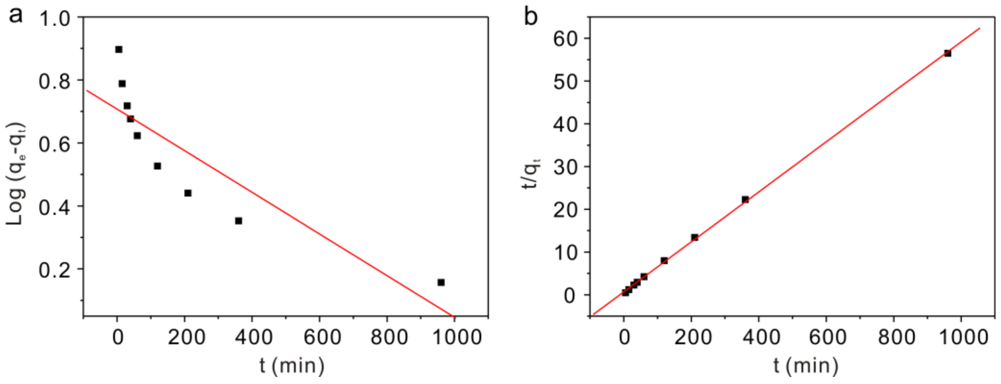

Fig. S10 Fitting of the adsorption kinetics of As(III) on the $MnFe_2O_4$ NCs by using pseudo-first-order kinetic model (a) and pseudo-second-order kinetic model (b). The fitted parameters are summarized in Table S2.

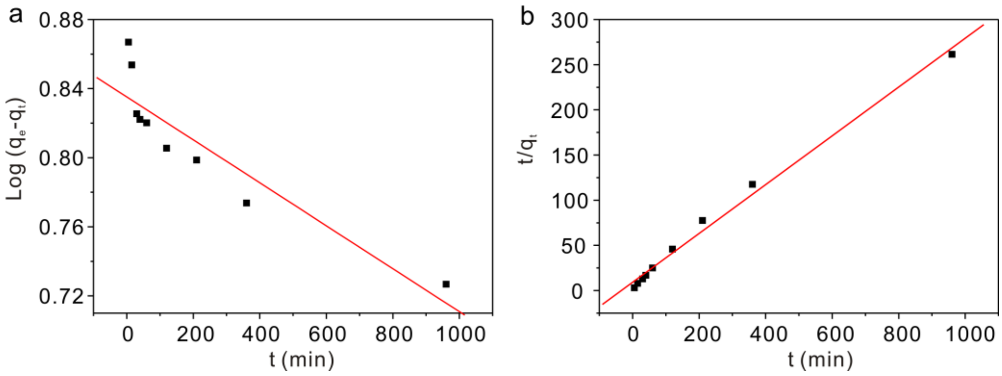

Fig. S11 Fitting of the adsorption kinetics of As(III) on the calcined $MnFe_2O_4$ NCs by using pseudo-first-order kinetic model (a) and pseudo-second-order kinetic model (b). The fitted parameters are summarized in Table S2.

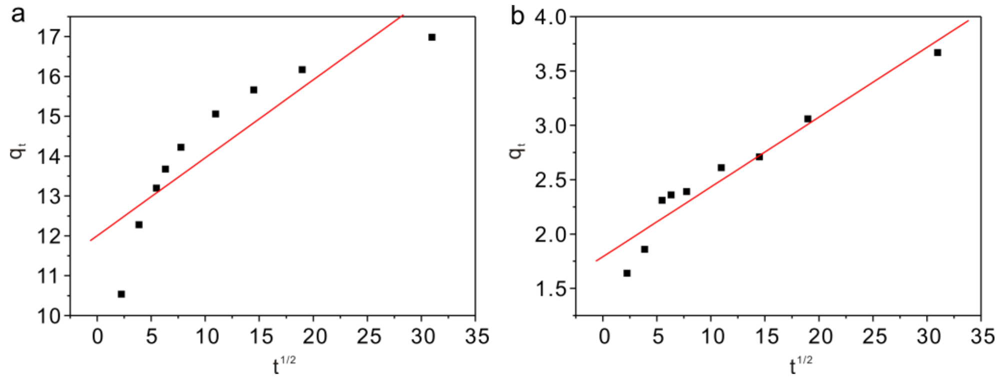

Fig. S12 Fitting of the adsorption kinetics of As(III) on the $MnFe_2O_4$ NCs (a) and the calcined $MnFe_2O_4$ NCs (b) by using the intra-particle pore diffusion model. The fitted parameters are summarized in Table S2.

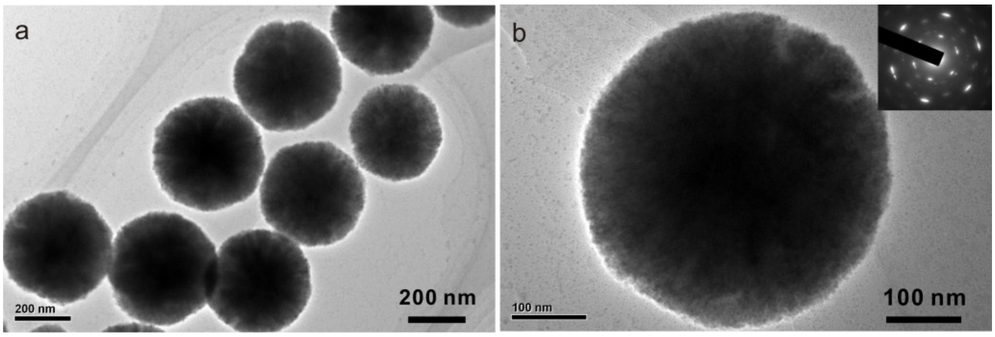

Fig. S13 TEM images of the regenerated $MnFe_2O_4$ NCs after 8 cycles of reuse at different magnifications. The inset is the corresponding SAED pattern.

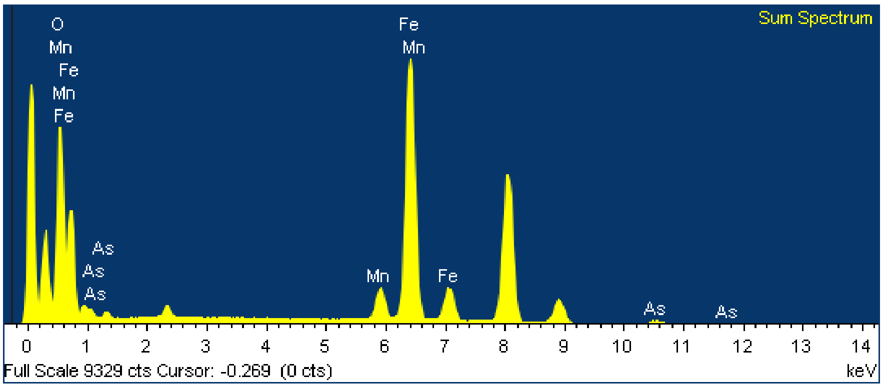

Fig. S14 EDX spectra of $MnFe_2O_4$ NCs after adsorbing As(III)

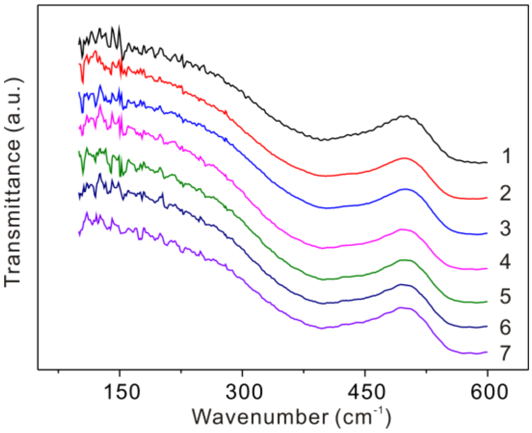

Fig. S15 Far-IR spectra of $MnFe_2O_4$ NCs (1) and $MnFe_2O_4$ NCs after treatment in aqueous solutions of six different As(III) concentrations, 1 mg L^{-1} (2), 10 mg L^{-1} (3), 20 mg L^{-1} (4), 30 mg L^{-1} (5), 40 mg L^{-1} (6), and 50 mg L^{-1} (7), respectively.

Table S1 Isotherm parameters for adsorption of As(III) on $MnFe_2O_4$ NCs and $MnFe_2O_4$ NCs calcined at 500°C.

	Langmuir isotherm			Freundlich isotherm			D-R isotherm		
Sample	q_{max} (mg g^{-1})	b (L mg^{-1})	R^2	K_f	1/n	R^2	K_{ads}	Q_m (mg g^{-1})	R^2
$MnFe_2O_4$ NCs	17.8	2.39	0.899	7.95	0.392	0.974	4.176×10^{-8}	17.83	0.837
Calcined $MnFe_2O_4$ NCs	3.45	18.85	0.939	2.535	0.291	0.944	1.55×10^{-8}	3.88	0.773

Table S2 Fitted parameters of As(III) adsorption kinetics and diffusion on $MnFe_2O_4$ NCs and $MnFe_2O_4$ NCs calcined at 500°C.

Sample	Pseudo-second-order		Pseudo-first-order		Intra-particle pore diffusion model	
	h (mg g^{-1} min^{-1})	R^2	k_{ads} (min^{-1})	R^2	K_i	R^2
$MnFe_2O_4$ NCs	1.52	0.9996	1.523×10^{-3}	0.775	0.1955	0.774
Calcined $MnFe_2O_4$ NCs	0.109	0.992	2.864×10^{-4}	0.833	0.0642	0.928

[1] Chen, H. M.; Chu, P. K.; He, J. H.; Hu, T.; Yang, M. Q. Porous magnetic manganese oxide nanostructures: Synthesis and their application in water treatment. *J. Colloid Interf. Sci.* **2011,** *359*, 68-74.

[2] Dhoble, R. M.; Lunge, S.; Bhole, A. G.; Rayalu, S., Magnetic binary oxide particles (MBOP): A promising adsorbent for removal of As (III) in water. *Water Res* **2011,** *45* (16), 4769-4781.